

## Rodlike micelles of dimethyloleylamine oxide in aqueous NaCl solutions, and their flexibility and size distribution

T. Imae and S. Ikeda

Department of Chemistry, Faculty of Science, Nagoya University, Chikusa, Nagoya, Japan

**Abstract:** Angular dependence of light scattering from aqueous NaCl solutions of dimethyloleylamine oxide has been measured in the presence of NaCl from  $5 \times 10^{-4}$  M to  $10^{-1}$  M at 25 °C. The molecular weight and radius of gyration of micelles increase with increasing micelle concentration and reach constant values, suggesting occurrence of the sphere-rod equilibrium dependent on the micelle concentration. With increasing NaCl concentration, rodlike micelles are larger in molecular weight and become longer. The micelles formed at NaCl concentrations higher than  $10^{-3}$  M are nearly monodisperse when the micelle concentration is high.

Rodlike micelles of dimethyloleylamine oxide in  $10^{-2}$  M and  $5 \times 10^{-2}$  M NaCl solutions have molecular weights of 4,760,000 and 6,900,000, respectively, and behave as semi-flexible or wormlike chains. In  $5 \times 10^{-2}$  M NaCl they have a contour length of 5750 Å and a persistence length of 1760 Å. These micelle parameters correspond to the end-to-end distance of 3780 Å and the number of Kuhn's statistical segments of 1.64. The large aggregation number of the rodlike micelles is induced by the strong cohesion of long hydrocarbon chains in solution, and their flexibility is caused by the hydration of amine oxide groups.

**Key words:** dimethyloleylamine oxide, rodlike micelles, light scattering, micelle size, wormlike chain.

### Introduction

Most nonionic surfactants form spherical micelles alone in aqueous solutions above the critical micelle concentration, even when some salt is present [1-8]. However, some of them can further associate into large or rodlike micelles, either at room or elevated temperatures, when the surfactant concentration exceeds the critical micelle concentration [9-16]. Hexaoxyethylene dodecyl ether [9, 10, 15] and hepta-oxyethylene cetyl ether [11, 12, 16] are found to form large micelles in water at room temperature. We can expect that nonionic surfactants can form rodlike micelles if the hydrophobicity is much stronger than the hydrophilicity. These properties of surfactant can be determined by the length of hydrocarbon chain relative to the size and hydration of polar head group.

Amine oxide is very hydrophilic and can constitute a good polar head group for nonionic surfactants at neutral pH. Dimethyldodecylamine oxide was first

prepared by Hoh et al. [17], and its amphipathic properties in aqueous solutions were investigated by the measurements of surface tension [18], light scattering [19-21] and hydrodynamic properties [22]. Dimethyldodecylamine oxide can form only spherical micelles in water and aqueous NaCl solutions, when the micelle concentration is dilute [19, 21]. Similarly, dimethyltetradecylamine oxide forms only spherical micelles in water [19].

In this paper we report the formation of rodlike micelles of dimethyloleylamine oxide,  $\text{CH}_3(\text{CH}_2)_7\text{CH}=\text{CH}(\text{CH}_2)_8\text{N}(\text{CH}_3)_2\text{O}$ , in aqueous NaCl solutions. Without added acid, the surfactant should behave as a nonionic. We measure light scattering in aqueous NaCl solutions of dimethyloleylamine oxide and observe normal behavior of its angular dependence, as long as the NaCl concentration is higher than  $10^{-4}$  M. In pure water and  $10^{-4}$  M NaCl solution, however, the angular dependence of light scattering has exhibited the strong effect of external interfer-

ence, and complicated analysis has been required to derive any micellar properties from the observed data [23]. Here we describe the results on light scattering in aqueous solutions of dimethyloleylamine oxide in the presence of  $5 \times 10^{-4} - 10^{-1}$  M NaCl, in which the effect of internal interference is more dominant than that of external interference, and we observe the formation of monodisperse rodlike micelles, which behave as wormlike chains.

## Experimental

### Materials

An aqueous solution containing  $(9.00 \pm 0.01)$  % dimethyloleylamine oxide was kindly supplied by Dr. F. Hoshino of Kao Soap Co., Inc., Wakayama. The dimethyloleylamine oxide was prepared from dimethyloleylamine by the reaction with  $H_2O_2$ . The concentration of the stock solution was determined by evaporating an aliquot of the solution and weighing its dry weight. Water was redistilled from alkaline  $KMnO_4$ . Special grade NaCl was ignited for two hours and stored in a desiccator until use. Solutions were prepared by diluting the stock solution with aqueous NaCl solutions and kept overnight at room temperature. The pH of the solutions was 7–8 and assured the nonionic nature of the surfactant.

### Measurements

Light scattering was measured on a Shimadzu Light Scattering Photometer PG-21, by using unpolarized light of a mercury lamp at 436 nm, as previously described [23]. A cylindrical cell put in a cell housing was filled with about  $35 \text{ cm}^3$  of solvent or solution, and the intensities of light scattered in the directions from  $30^\circ$  to  $150^\circ$  were measured. The apparatus was calibrated by using purified benzene.

The solvents and solutions for light scattering measurements were directly filtered into the cylindrical cell under pressure through Millipore filter GSWP, having a pore size of  $0.22 \mu\text{m}$  and a diameter of  $47 \text{ mm}\phi$ . The filtration was repeated at least five times for a solvent or a solution, until it was dust-free and had constant dissymmetry. The filter had been washed four times, each time by  $50 \text{ cm}^3$  of redistilled water, in order to remove water-soluble contaminants: the contaminants had absorption in the ultraviolet region and could be detected spectrophotometrically.

The concentration of solution after filtration was determined spectrophotometrically. The optical density at the maximum wavelength of a band around 190–220 nm was measured for each solution, and its concentration was determined by the calibration curve of optical density. Results on measurement of absorption spectra of dimethyloleylamine oxide in aqueous NaCl solutions will be reported elsewhere.

The refractive index increment was measured on a Shimadzu Differential Refractometer DR-3 of the Brice type at the wavelength of 436 nm of a mercury lamp. The calibration of the apparatus was performed by aqueous solutions of NaCl.

Temperature was kept at  $25 \pm 0.05^\circ\text{C}$ , by circulating water of constant temperature through the cell housing of each apparatus.

## Results

### a) Light scattering

The specific refractive index increment of solutions of a constant NaCl concentration was constant over

the surfactant concentrations up to  $0.3 \times 10^{-2} \text{ g cm}^{-3}$ , and its values are given in table 1.

Table 1. Characteristics of rodlike micelles of dimethyloleylamine oxide in aqueous NaCl solutions

$C_s$ (M)	$(\partial\bar{n}/\partial c)_{C_s}$ ( $\text{cm}^3 \text{ g}^{-1}$ )	$M_w$ ( $10^4$ )	$m_w$	$(\overline{R_G^2})_s^{1/2}$ ( $\text{\AA}$ )	$L$ ( $\text{\AA}$ )	$L/m_w$ ( $\text{\AA}$ )
$5 \times 10^{-4}$	0.162	147	4720	(560)*	1940	0.41
$1 \times 10^{-3}$	0.161 <sub>5</sub>	270	8670	(850)*	2940	0.34
$1 \times 10^{-2}$	0.161 <sub>5</sub>	476	15300	1120	3880	0.25
$5 \times 10^{-2}$	0.161	690	22100	1270	4400	0.20
$1 \times 10^{-1}$	0.160					

\* possibly subject to some effect of external interference

Solutions in  $5 \times 10^{-2}$  M and  $10^{-1}$  M NaCl developed opalescence portending imminent emulsification, which perturbed accurate observation of deflection of the slit image at high surfactant concentrations. Hence, the values observed at lower surfactant concentrations are given in table 1. The range of these surfactant concentrations is, however, still within the range for light scattering measurements.

Figure 1 shows the variations of reduced scattering intensity in the  $90^\circ$  direction,  $R_{90}$ , and angular dissymmetry,  $z_{45} = R_{45}/R_{135}$ , with surfactant concentration at various NaCl concentrations. In the presence of  $10^{-1}$  M NaCl, the solutions underwent liquid-liquid phase separation at surfactant concentrations above  $0.08 \times 10^{-2} \text{ g cm}^{-3}$ . The reduced scattering intensity increases with increasing surfactant concentration beyond the critical micelle concentration of  $0.003 \times 10^{-2} \text{ g cm}^{-3}$  (or  $9.6 \times 10^{-5}$  M) for all NaCl solutions, and the extent of its increase is greater for solutions with higher NaCl concentrations. The curve is convex upward at low NaCl concentrations and turns convex downward at high NaCl concentrations.

While the dissymmetry passes a maximum at a low micelle concentration in dilute NaCl solutions, it reaches a constant value in more concentrated NaCl solutions after gradual initial increase above the critical micelle concentration.

The intensity of light scattered in the direction,  $\theta$ , from a micellar solution irradiated by unpolarized light can be represented by

$$\frac{K(c-c_0)}{R_\theta - R_\theta^0} - \frac{1}{M_w P(\theta)} + 2B(c-c_0) \quad (1)$$

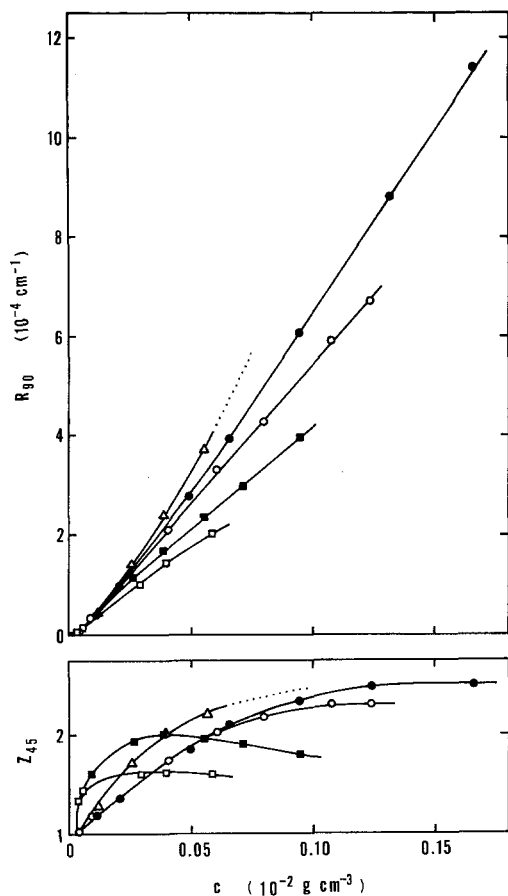


Fig. 1. The reduced scattering intensity in the  $90^\circ$  direction (upper) and the angular dissymmetry at  $45^\circ$  (lower) of scattered light as a function of surfactant concentration. NaCl concentration (M):  $\square$ ,  $5 \times 10^{-4}$ ;  $\blacksquare$ ,  $10^{-3}$ ;  $\circ$ ,  $10^{-2}$ ;  $\bullet$ ,  $5 \times 10^{-2}$ ;  $\triangle$ ,  $10^{-1}$ . Dotted parts indicate that the solutions undergo phase separation

where  $R_\theta$  and  $R_\theta^0$  are the reduced scattering intensities at a surfactant concentration,  $c$  ( $\text{g cm}^{-3}$ ), and at the critical micelle concentration,  $c_o$ , respectively.  $M_w$  is the weight-average molecular weight of micelles,  $P(\theta)$  the particle scattering factor, and  $B$  the second virial coefficient.

The optical constant,  $K$ , is given by

$$K = \frac{2\pi^2 \tilde{n}_o^2 (\partial \tilde{n} / \partial c)_C^2 C_s}{N_A \lambda^4} \quad (2)$$

where  $\tilde{n}_o$  and  $(\partial \tilde{n} / \partial c)_C$  are, respectively, the refractive index of solvent and the specific refractive index increment of solution at a constant NaCl concentration,  $C_s$  (M or mole  $\text{dm}^{-3}$ ).  $\lambda$  is the wavelength of light in vacuo, 436 nm, and  $N_A$  is the Avogadro number.

For small scattering angles, the particle scattering factor reduces to

$$\left( \frac{1}{P(\theta)} \right)_{\mu: \text{small}} = 1 + \frac{1}{3} \mu^2 (\overline{R_G^2})_s \quad (3)$$

with

$$\mu = \frac{4\pi \tilde{n}_o}{\lambda} \sin \left( \frac{\theta}{2} \right) \quad (4)$$

irrespective of particle shape, where  $(\overline{R_G^2})_s$  is the light-scattering-average mean-square radius of gyration of micelles [24, 25]. Eq. (3) is applicable for  $200 \text{ \AA} < (\overline{R_G^2})_s^{1/2} < 2000 \text{ \AA}$  [26].

The reciprocal angular envelope of light scattering is shown in figure 2 for solutions in  $10^{-2} \text{ M NaCl}$ . At low micelle concentrations the Zimm plot increases linearly with an increase in scattering angle but the

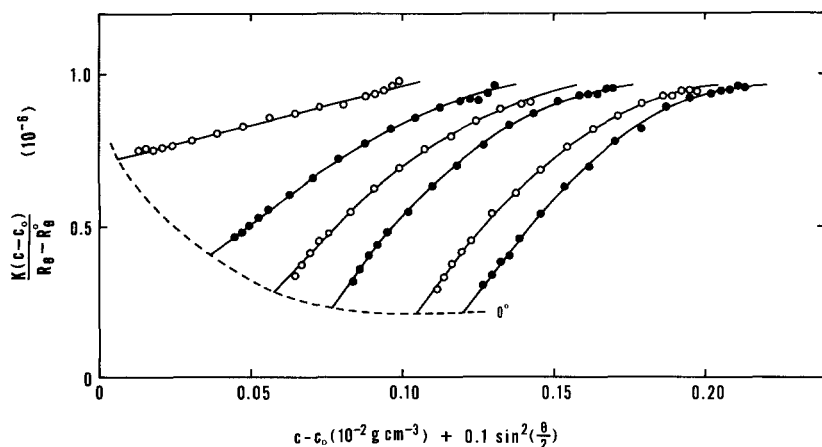


Fig. 2. The Zimm plots of light scattering for  $10^{-2} \text{ M NaCl}$  solution. Micelle concentration ( $10^{-2} \text{ g cm}^{-3}$ ), from left to right: 0.006, 0.038, 0.058, 0.077, 0.105, and 0.121

angular dependence is low. However, at high micelle concentrations it is convex upward and the initial slope of angular dependence is steeper. In such a case, it is not always ready to extrapolate exactly the angular dependence to zero scattering angle, because of possible curvature at low angles. However, it has been assured [27] that the extrapolation can be effected accurately even from the region of angles not lower than  $30^\circ$ , as long as the molecular weight does not exceed  $6 \times 10^6$  appreciably. This condition is fulfilled for the present micelles, as will be shown below.

### b) Micelle parameters

Figure 3 (a) illustrates the Debye plots at zero scattering angle for aqueous NaCl solutions of micelles, which give the reciprocal of apparent molecular weight. All of them decrease with increasing concentration, indicating that small spherical micelles are formed at the critical micelle concentration and they associate further into large micelles with increasing

micelle concentration. Thus the concentration-dependent equilibrium holds between the small micelles and the large micelles.

In  $5 \times 10^{-4}$  M and  $10^{-3}$  M NaCl solutions the effect of the second virial coefficient of the large micelles is manifest, thus giving minima on the Debye plots: for  $10^{-3}$  M NaCl the second virial coefficient can be assigned to be  $2B = 2.14 \times 10^{-4} \text{ cm}^{-3} \text{ g}^{-1}$ , and the correction of this term is applied for the Debye plots so as to derive the weight-average molecular weight of the large micelles at finite concentrations. At higher NaCl concentrations, the second virial coefficient would be very small and is negligible. Then the reciprocal of the Debye plot can be identified with the weight-average molecular weight of micelles. The values of  $M_w$  at high micelle concentrations, which should be essentially equal to those of molecular weight of the large micelle, are listed in Table 1, together with those of the weight-average micelle aggregation number,  $m_w = M_w/311.6$ .

The root-mean-square radius of gyration,  $(\overline{R_G^2})^{1/2}$ , is obtained from the initial slope of the Zimm plot, and its values are given in figure 3 (b) as a function of micelle concentration. It will be more likely that the effect of external interference is still operative at lower NaCl concentrations, so that the values of  $(\overline{R_G^2})^{1/2}$  might be subject to some errors in  $5 \times 10^{-4}$  M and  $10^{-3}$  M NaCl. Apart from this effect, however, the values of  $(\overline{R_G^2})^{1/2}$  in each NaCl solution gradually increase with the micelle concentration and then become constant at high micelle concentrations. This feature is consistent with that observed for  $M_w$ : the equilibrium between two kinds of micelles shifts from small to large micelles, as the micelle concentration increases. The values of  $(\overline{R_G^2})^{1/2}$  obtained at high micelle concentrations, which should be essentially equal to the radius of gyration of the large micelle, are also listed in Table 1.

The values of  $(\overline{R_G^2})^{1/2}$  are approximately proportional to those of molecular weight,  $M_w$ . This suggests that the shape of the large micelles is rodlike. The constant values of angular dissymmetry at high micelle concentrations, 2.3 for  $10^{-2}$  M NaCl solution and 2.5 for  $5 \times 10^{-2}$  M NaCl solution, are close to the theoretical value of 2.41 for a rigid rod. The curvature convex upward of the Zimm plots at high micelle concentrations is also characteristic of rod particles [25, 28]. If large micelles were rigid rods, their length should be given by  $L = 12^{1/2} (\overline{R_G^2})^{1/2}$ . The values of rigid-rod length,  $L$ , and molecular pitch,  $L/m_w$ , are given in table 1. With increasing NaCl concentration, the aggregation number and the length of rodlike micelles increase.

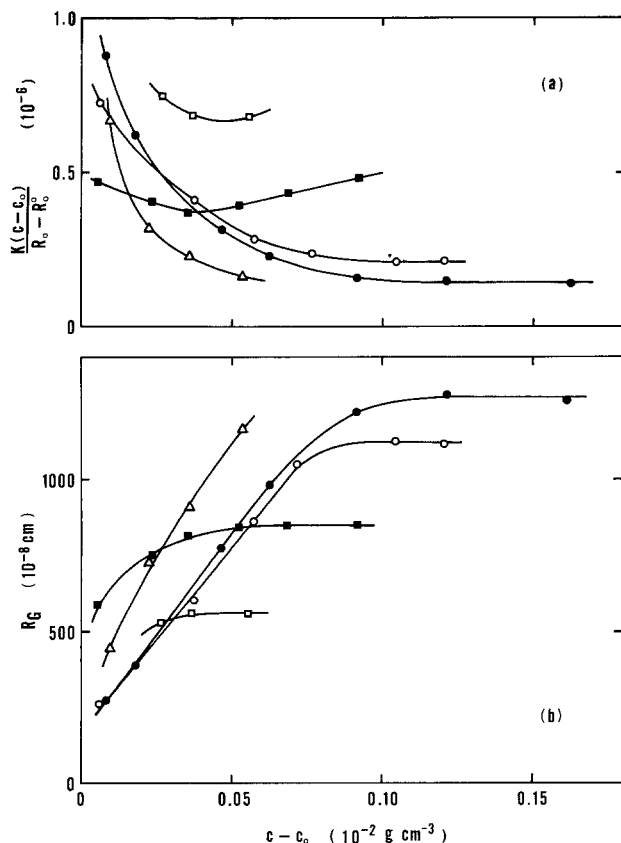


Fig. 3. (a) The Debye plots for light scattering in the  $0^\circ$  direction and (b) the concentration dependence of the radius of gyration. Symbols have the same meanings as given in figure 1

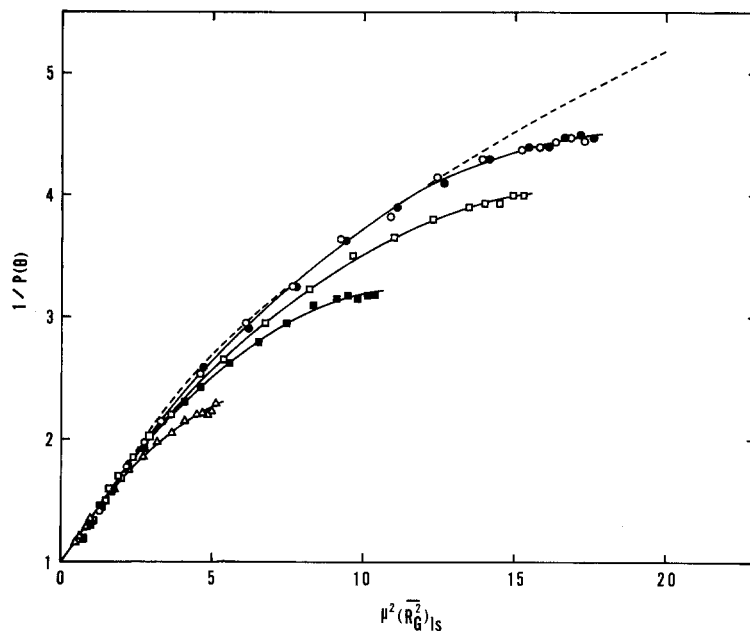


Fig. 4. The inverse scattering factor of light scattering as a function of  $\mu^2(\overline{R_G^2})_l$  for  $10^{-2}$  M NaCl solution. Micelle concentration ( $10^{-2}$  g  $\text{cm}^{-3}$ ):  $\Delta$ , 0.038;  $\blacksquare$ , 0.058;  $\square$ , 0.077;  $\bullet$ , 0.105;  $\circ$ , 0.121. ---, calculated for rigid rods

The particle scattering factor of a rigid rod having a length  $L$  is given by [29, 30].

$$P(\theta) = \frac{1}{X} \int_0^{2X} \frac{\sin w}{w} dw - \left( \frac{\sin X}{X} \right)^2 \quad X = \frac{1}{2} \mu L \quad (5)$$

The observed values of the inverse scattering factor for solutions in  $10^{-2}$  M NaCl are plotted against  $\mu^2(\overline{R_G^2})_l$  in figure 4, using the values of  $(\overline{R_G^2})_l$  obtained from the initial slope. The calculated curve for rigid rods is also drawn according to equation (5). Generally, the agreement between observed and calculated values is good, supporting the thin rod model. However, at low micelle concentrations, the observed values deviate from the calculated curve in such a way that the observed intensity is stronger. This must be ascribed to the polydispersity of the micelles at low concentrations, if the rodlike micelles have a common cross-section [31].

Assuming that the polydispersity comes from different lengths of rod particles with a common diameter, the inverse scattering factor at large scattering angles can be represented by [31]

$$\left( \frac{1}{P(\theta)} \right)_{X: \text{large}} = M_w \left( \frac{2}{\pi^2 M_n} + \frac{\mu}{\pi d} \right) \quad (6)$$

where  $M_n$  is the number-average micelle molecular weight. Here the linear molecular weight density,

$d = M_i/L_i$ , is the molecular weight per unit length of each rod,  $i$ , and it should be common to all the rodlike micelles.

According to equation (6), the value of  $d$  at each micelle concentration can be obtained from the slope at large scattering angles in the plot of  $1/P(\theta)$  against  $\mu$ , and the value of  $1/M_n$  can be derived from its extrapolation to zero scattering angle. Figure 5 gives such plots for different micelle concentration in the presence of  $10^{-2}$  M NaCl.

Figure 6 gives the dependence of the  $d$  value on the micelle concentration. The value of  $d$  decreases with increasing micelle concentration and approaches or attains a constant value. However, this decrease must be taken with some reservation, since equation (6) assumes that all the micelles are rodlike and very long, but the micellar solutions should contain spherical micelles together. Nevertheless, in aqueous solutions of  $10^{-2}$  M or lower NaCl concentrations, the value of  $d$  reduces to  $1200 \text{ \AA}^{-1}$  at high micelle concentrations, where the contribution of spherical micelles would be negligible.

Figure 7 shows the values of  $1/M_n$  and  $M_w/M_n$ , the latter of which is a measure of polydispersity of the rodlike micelles. Both parameters sharply decrease with increasing surfactant concentration at low micelle concentrations; they become constant at high micelle concentrations, just like the parameters,  $1/M_w$  and  $(\overline{R_G^2})_l^{1/2}$ , in figure 3. The constant values of both para-

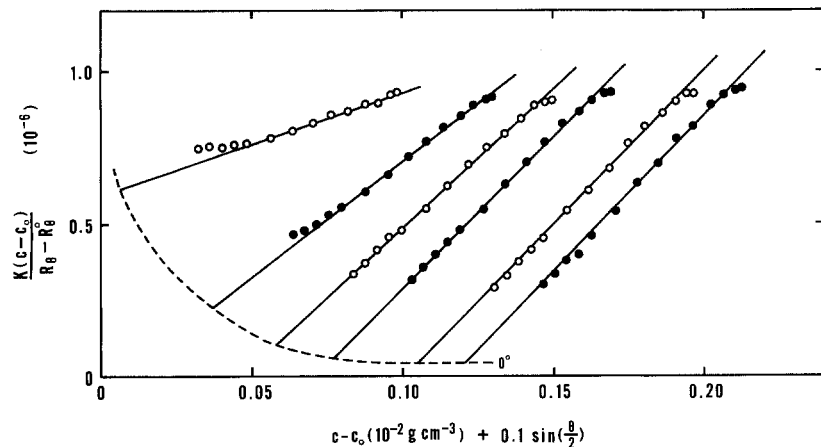


Fig. 5. The reciprocal angular envelope of light scattering as a function of  $\sin(\theta/2)$  for  $10^{-2}$  M NaCl solution. Micelle concentration ( $10^{-2}$  g  $\text{cm}^{-3}$ ), from left to right; 0.006, 0.038, 0.058, 0.077, 0.105, and 0.121

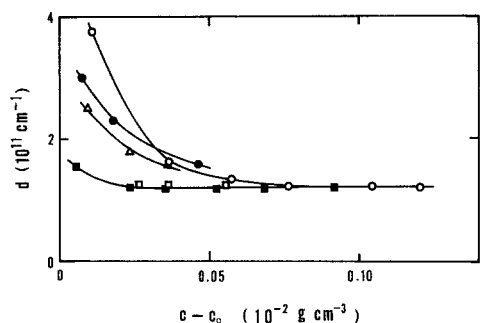


Fig. 6. The dependence of the linear molecular weight density  $d$  on the micelle concentration. Symbols have the same meanings as given in figure 1

meters decrease with an increase in NaCl concentration. At lower NaCl concentrations, these values would be subject to some errors arising from the external interference.

It may be noticed that the value of  $M_w/M_n$  is close to unity in the solutions of NaCl concentrations higher than  $10^{-3}$  M and at micelle concentrations more concentrated than  $0.09 \times 10^{-2}$  g  $\text{cm}^{-3}$ . In these solutions the rodlike micelles have a very narrow size distribution. At lower micelle concentrations the polydispersity of the rodlike micelles is rather high, but this would come from the effect of spherical micelles existing together.

c) Treatment as wormlike chains

As shown in figure 8, the observed values of the inverse scattering factor for aqueous solutions in  $5 \times 10^{-2}$  M NaCl deviate upward at high micelle concentrations from the calculated curve for rigid rods. If the rodlike micelles were polydisperse, equation (6) could be applied to obtain the number-average molecular

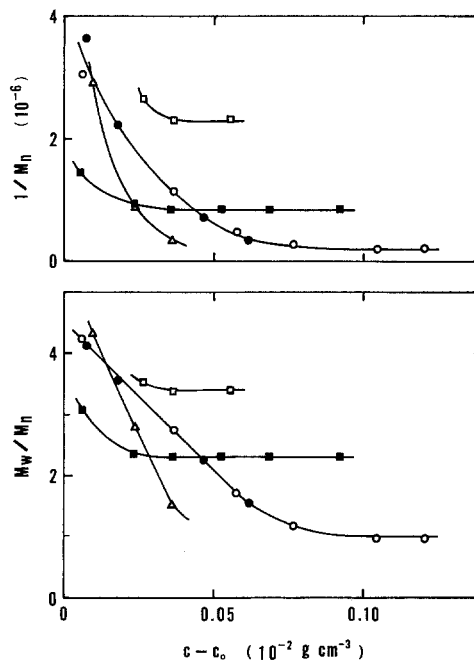


Fig. 7. Variations of the inverse number-average molecular weight (upper) and the polydispersity (lower) with the micelle concentration. Symbols have the same meanings as given in figure 1

weight. However, negative values of  $M_n$  result from such a treatment as above. Thus, instead of being polydisperse, the rodlike micelles must have some flexibility in  $5 \times 10^{-2}$  M NaCl.

As can be seen in Table 1, the average radius of gyration of the rodlike micelles is not strictly proportional to the molecular weight. The flexibility of the rodlike micelles is thus exhibited in the molecular pitch,  $L/m_w$ , decreasing with increasing aggregation number.

Such a flexible rodlike micelle can be treated in terms of the wormlike chain of Kratky and Porod.

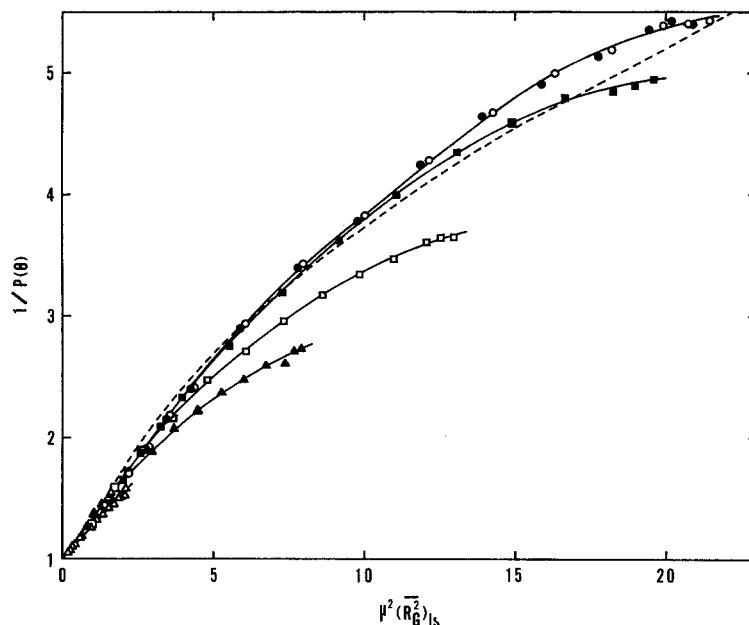


Fig. 8. The inverse scattering factor of light scattering as a function of  $\mu^2(\overline{R_G^2})_s$  for  $5 \times 10^{-2}$  M NaCl solution. Micelle concentration ( $10^{-2}$  g cm $^{-3}$ ):  $\Delta$ , 0.018;  $\blacktriangle$ , 0.047;  $\square$ , 0.063;  $\blacksquare$ , 0.092;  $\circ$ , 0.121;  $\bullet$ , 0.163. ---, calculated for rigid rods

[32]. If the contour length and persistence length of a wormlike chain are represented by  $L_c$  and  $a$ , respectively, its mean-square radius of gyration,  $\langle s^2 \rangle_o$ , and its mean-square end-to-end distance,  $\langle r^2 \rangle_o$ , are given by [28, 32].

$$\frac{\langle s^2 \rangle_o}{a^2} = \frac{L_c}{3a} - 1 + \frac{2a}{L_c} \left[ 1 - \frac{a}{L_c} (1 - e^{-L_c/a}) \right] \quad (7)$$

$$\frac{\langle r^2 \rangle_o}{2a^2} = \frac{L_c}{a} - 1 + e^{-L_c/a} \quad (8)$$

where the suffix, o, means that they stand for the unperturbed chains, i. e., the chains without the excluded volume effect.

The contour length,  $L_c$ , is related to the molecular weight,  $M$ , by

$$L_c = M/M_L \quad (9)$$

where  $M_L$  is the molecular weight per unit chain length. Here the symbols,  $\langle s^2 \rangle_o$ ,  $M$  and  $M_L$ , are used to emphasize the quantities corresponding to  $(\overline{R_G^2})_s$ ,  $M_w$  and  $d$ , respectively, for a monodisperse rodlike micelle.

As seen from figure 6, we can see  $M_L = 1200 \text{ \AA}^{-1}$ . Then the micelle parameters observed at micelle concentrations higher than  $0.1 \times 10^{-2}$  g cm $^{-3}$  in  $10^{-2}$  M and  $5 \times 10^{-2}$  M NaCl can be assigned to those of the monodisperse rodlike micelles. By using equations (7) – (9) we have the values of these parameters as the wormlike

Table 2. Parameters of rodlike micelles as wormlike chains

$C_s$ (M)	$\langle s^2 \rangle_o^{1/2}$ ( $\text{\AA}$ )	$L_c$ ( $\text{\AA}$ )	$a$ ( $\text{\AA}$ )	$L_c/2a$	$\langle r^2 \rangle_o^{1/2}$ ( $\text{\AA}$ )
$1 \times 10^{-2}$	1120	3970	17400	0.11	3820
$5 \times 10^{-2}$	1270	5750	1760	1.64	3780

chains, as shown in table 2. It is observed that, while the rodlike micelles in  $10^{-2}$  M NaCl are relatively extended, the longer rodlike micelles in  $5 \times 10^{-2}$  M NaCl are considerably flexible.

## Discussion

### a) Sphere-rod equilibrium

From the dependence on the micelle concentration of molecular weight and radius of gyration, we may conclude that micelles of dimethyloleylamine oxide are subject to a sphere-rod equilibrium in aqueous NaCl solutions. That is, small spherical micelles would be formed at the critical micelle concentration, and with increasing micelle concentration they associate together into large rodlike micelles.

Similar sphere-rod equilibria of micelles dependent on micelle concentration were found for ionic surfactants such as sodium dodecyl sulfate and dodecyltrimethylammonium halides in concentrated NaCl and NaBr solutions [33–37]. Such a sphere-rod equilib-

rium of ionic micelles occurs when the ionic strength exceeds a threshold value characteristic of the surfactant species. The threshold ionic strength is usually rather high. This indicates that the electrostatic effect of ionic micelles is sufficiently suppressed by the added salt so that the micelles behave as if they are uncharged.

While dimethyldodecylamine oxide forms only spherical micelles even in 0.20 M NaCl [21], micelles of dimethyloleylamine oxide are subject to a sphere-rod equilibrium in aqueous solutions of NaCl concentrations as dilute as  $10^{-4}$  M and even in water [23]. Thus the rodlike micelles are more stabilized as compared with the spherical micelles, when the hydrocarbon chain of the surfactant molecule is longer. This observation is consistent with our idea of geometrical adaptation that the rodlike micelles are more stable when the polar head group of the surfactant molecule or ion is smaller and the chain length of its hydrocarbon part is longer [33]. Furthermore, owing to the higher hydrophobicity of oleyl group, the aggregation number of rodlike micelles reaches considerably high values, ranging from 5,000 to 20,000, at very low NaCl concentrations.

#### *b) Size distribution of micelles*

At low micelle concentrations, polydispersity of micelle size is generally manifest, which is mostly attributable to the effect of coexistent spherical micelles. The polydispersity of micelles is, however, observed even at high micelle concentrations in  $5 \times 10^{-4}$  M and  $10^{-3}$  M NaCl, where it is independent of the micelle concentration. This may be attributable to the effect of external interference, which is stronger at lower NaCl concentrations and at higher micelle concentrations.

In  $10^{-2}$  M and  $5 \times 10^{-2}$  M NaCl, the polydispersity of micelles at high concentrations disappears, indicating that the rodlike micelles are monodisperse. The high polydispersity observed at lower micelle concentrations can be attributed to the coexistence of spherical micelles. It has been claimed on the basis of the isodesmic association mechanism [38–41] that the rodlike micelles are polydisperse, and then the polydispersity index,  $M_w/M_n$ , should increase monotonously from 1 to 2 with increasing micelle concentration. However, the present results give large values of this index at intermediate micelle concentrations and, therefore, cannot be explained by this mechanism. Rather they can be considered to give evidence for the equilibrium between small spherical micelles and large rodlike micelles.

More direct support for the monodispersity of rodlike micelles of nonionic and ionic surfactants were provided by the measurements of membrane osmometry and light scattering. By means of these methods Attwood et al. [42] found that the polydispersity index,  $M_w/M_n$ , was 1.10 or less for aqueous solutions of hexaoxyethylene dodecyl ether and nonaoxyethylene cetyl ether, indicating that the micelles were monodisperse. Birdi [43] arrived at a similar conclusion by applying the same procedures for 0.025 M KBr solutions of cetyltrimethylammonium bromide and aqueous solutions of polyoxyethylene nonylphenyl ether.

Our previous light scattering experiments on 0.80 M sodium halide solutions of sodium dodecyl sulfate at an elevated temperature indicated a concentration-dependent sphere-rod equilibrium of the micelles [35]. It is known that Adams' analysis of the weight-average molecular weight of self-associating solutes as a function of concentration can provide the number-average molecular weight [44]. By means of this method, we obtained the polydispersity of the micelles as a function of concentration and found that the micelles became monodisperse at high micelle concentrations. Applying the same analysis for the present results, we can arrive at the same conclusion that the monodisperse rodlike micelles of dimethyloleylamine oxide are formed in  $10^{-2}$  M or more concentrated NaCl solutions.

#### *c) Structure and flexibility of rodlike micelles*

As shown in figure 6, a limiting value,  $1200 \text{ \AA}^{-1}$ , can be assigned to the molecular weight per unit length,  $d$ , for the rodlike micelles. This indicates that the rodlike micelles have an identical cross-section, irrespective of NaCl concentration and also of micelle concentration. The rodlike micelles would have a structure consisting of a stack of disk-like layers, as shown in figure 9 (a); each layer is composed of surfactant molecules radially arranged, putting their amine oxide groups outside. If the layer has a thickness of 6 Å, then the observed  $d$  value should lead to the structure of such a layer having a molecular weight, 7200, thus containing 23 molecules in it. This number of molecules, 23, can be well compared with the value, 15, for dodecyldimethylammonium chloride [33].

If an oleyl group is extended, the length of a dimethyloleylamine oxide molecule would reach about 30 Å, and the rodlike micelles should have a diameter as thick as 60 Å. Based on the values given in table 2, we can illustrate the rodlike micelles in  $5 \times 10^{-2}$  M NaCl, as shown in figure 9 (b).



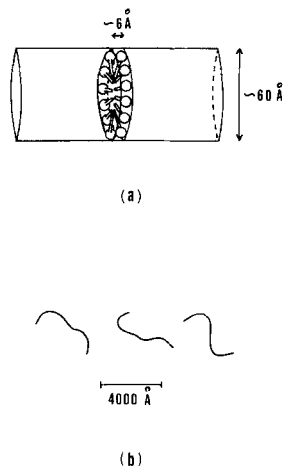


Fig. 9. (a) The partial cross-sectional structure of a rodlike micelle and (b) the wormlike character of rodlike micelles in  $5 \times 10^{-2}$  M NaCl

Flexibility of rodlike micelles was first suggested by Elworthy and Macfarlane [11], who measured angular dissymmetry of light scattering and specific viscosity of aqueous solutions of hexaoxyethylene cetyl ether and of heptaoxyethylene cetyl ether. They reached the conclusion that the rodlike micelles of hexaoxyethylene cetyl ether would behave more like random coils than those of heptaoxyethylene cetyl ether.

Strong evidence for the flexibility of rodlike micelles was also given for some ionic surfactants in concentrated salt solutions. Stigter [45] analyzed the data of intrinsic viscosity of dodecylammonium chloride in NaCl solutions and derived a flexible rod model. Ikeda et al [33] observed the molecular pitch,  $L/m_w$ , of rodlike micelles of dodecyltrimethylammonium chloride in NaCl solutions, which decreased with increasing micelle aggregation number, and ascribed this decrease to their flexibility. Later, Ozeki and Ikeda [46] measured the intrinsic viscosity of the micellar solutions and observed that the exponent of the Mark-Houwink equation was, at most, 1.3, which should be as high as 1.8 if the micelles were rigid rods. They further noticed that the exponent decreased to 0.6 for the micelles having molecular weights higher than  $10^6$ , indicating increased flexibility.

Appell et al. [47, 48] measured light scattering and magnetic birefringence of aqueous NaBr solutions of cetylpyridinium bromide and found its rodlike micelles to behave as wormlike chains having a persistence length as short as 200 Å. We have found that the persistence length of the rodlike micelles of dimethyl-

oleylamine oxide is much longer, in spite of nearly the same number of carbon atoms in hydrocarbon chains. Thus the micelles of dimethyloleylamine oxide are much more rigid than those of cetylpyridinium bromide. Since amine oxide group is strongly hydrophilic, we can infer that hydration of amine oxide group can confer rigidity on the rodlike micelles, as Elworthy and Macfarlane [11] suggested for the higher rigidity in hexaoxyethylene cetyl ether.

#### Acknowledgement

We would like to acknowledge Dr. Kenichi Hattori for drawing our attention to the characteristic properties of aqueous solutions of dimethyloleylamine oxide, and Dr. Fumio Hoshino for kindly supplying to us the valuable sample of dimethyloleylamine oxide.

#### References

1. Kushner LM, Hubbard WD (1954) *J Phys Chem* 58:1163
2. Becher P (1961) *J Colloid Sci* 16:49
3. Becher P (1962) *J Colloid Sci* 17:325
4. Schick MJ, Atlas SM, Eirich FR (1962) *J Phys Chem* 66:1326
5. Elworthy PH, Macfarlane CB (1962) *J Chem Soc* 537
6. Elworthy PH, Florence AT (1965) *Kolloid Z Z Polymere* 204:105
7. ElEini DID, Barry BW, Rhodes CT (1976) *J Colloid Interface Sci* 54:348
8. Tanford C, Nozaki Y, Rohde F (1977) *J Phys Chem* 81:1555
9. Balmбра RR, Clunie JS, Corkill JM, Goodman JF (1962) *Trans Faraday Soc* 58:1661
10. Balmбра RR, Clunie JS, Corkill JM, Goodman JF (1964) *Trans Faraday Soc* 60:979
11. Elworthy PH, Macfarlane CB (1963) *J Chem Soc* 907
12. Elworthy PH, McDonald C (1964) *Kolloid Z Z Polymere* 195:16
13. Herrmann KW, Bruchmiller JG, Courchene WL (1966) *J Phys Chem* 70:2909
14. Corkill JM, Goodman JF, Walker T (1967) *Trans Faraday Soc* 63:759
15. Ottewill RH, Storer CC, Walker T (1967) *Trans Faraday Soc* 63:2796
16. Attwood D (1968) *J Phys Chem* 72:339
17. Hoh LK, Barlow DO, Chadwick AF, Lake DB, Sheeran SR (1963) *J Amer Oil Chem Soc* 40:268
18. Ikeda S, Tsunoda M, Maeda H (1978) *J Colloid Interface Sci* 67:336
19. Herrmann KW (1962) *J Phys Chem* 66:295
20. Corkill JM, Herrmann KW (1963) *J Phys Chem* 67:934
21. Ikeda S, Tsunoda M, Maeda H (1979) *J Colloid Interface Sci* 70:448
22. Courchene WL (1964) *J Phys Chem* 68:1870
23. Imae T, Ikeda S (1984) *J Colloid Interface Sci* 98:363
24. Zimm BH (1948) *J Chem Phys* 16:1099
25. Geiduschek EP, Holtzer A (1958) *Advan Biol Med Phys* 6:431
26. Tanford C (1961) *Physical Chemistry of Macromolecules*, Chap 5:305 Wiley
27. Froelich D, Strazielle C, Bernardi G, Benoit H (1963) *Biophys J* 3:115
28. Benoit H, Doty P (1953) *J Phys Chem* 57:958

29. Debye P, Anacker EW (1950) *J Phys Colloid Chem* 55:644
30. Doty P, Steiner RF (1950) *J Chem Phys* 18:1211
31. Holtzer A (1955) *J Polymer Sci* 17:432
32. Kratky O, Porod G (1949) *Rec Trav Chim* 68:1106
33. Ikeda S, Ozeki S, Tsunoda M (1980) *J Colloid Interface Sci* 73:27
34. Hayashi S, Ikeda S (1980) *J Phys Chem* 84:744
35. Ikeda S, Hayashi S, Imae T (1981) *J Phys Chem* 85:106
36. Ozeki S, Ikeda S (1982) *J Colloid Interface Sci* 87:424
37. Ozeki S, Ikeda S (1984) *Colloid Polymer Sci* 262:409
38. Mukerjee P (1972) *J Phys Chem* 76:565
39. Tausk RJM, Overbeek JThG (1974) *Biophys Chem* 2:175
40. Missel PJ, Mazer NA, Benedek GB, Young CY, Carey M (1980) *J Phys Chem* 84:1044
41. Porte G, Appell J (1981) *J Phys Chem* 85:2511
42. Attwood D, Elworthy PH, Kayne SB (1970) *J Phys Chem* 74:3529
43. Birdi KS (1972) *Kolloid Z Z Polymere* 250:731
44. Adams ET Jr (1965) *Biochemistry* 4:1646
45. Stigter D (1966) *J Phys Chem* 70:1323
46. Ozeki S, Ikeda S (1981) *J Colloid Interface Sci* 77:219
47. Porte G, Appell J, Poggi Y (1980) *J Phys Chem* 84:3105
48. Appell J, Porte G, Poggi Y (1982) *J Colloid Interface Sci* 87:492

Received December 21, 1983;  
accepted February 17, 1984

Authors' address:

Toyoko Imae and Shoichi Ikeda  
Department of Chemistry  
Faculty of Science  
Nagoya University  
Chikusa, Nagoya 464, Japan